J. Cent. South Univ. (2016) 23: 258−268
DOI: 10.1007/s11771-016-3069-1

Springer

Inhibition effect of 2-amino-5-ethyl-1, 3, 4-thiadiazole on corrosion behaviour of austenitic stainless steel type 304 in dilute HCl solution

Roland T. Loto[1, 2], Cleophas A. Loto[1, 2], Abimbola P. Popoola[2], Tatiana Fedotova[2]

1. Department of Mechanical Engineering, Covenant University, Ota, Ogun State, Nigeria;
2. Department of Chemical, Metallurgical & Materials Engineering, Tshwane University of Technology, Pretoria, South Africa

Abstract: The corrosion inhibition of type 304 austenitic stainless steel by 2-amino-5-ethyl-1, 3, 4-thiadiazole (TTD) compound and the electrochemical behaviour in dilute HCl solution were investigated through potentiodynamic polarization test, mass loss techniques and potential measurements. The results show that the organic derivative is highly effective with a maximum inhibition efficiency of 70.22% from mass loss analysis, while 74.2% is obtained from polarization tests. Observation of the scanning electron micrographs shows the absence of corrosion products due to electrochemical influence of TTD on the surface morphology of the steel. X-ray diffractometry reveals the absence of phase compounds and complexes on the steel samples after exposure. TTD adsorption on the steel surface obeys the Langmuir, Frumkin and Freundlich adsorption isotherms. Corrosion thermodynamic calculations reveal the inhibition mechanism occurs through chemisorption process and results from statistical analysis depict the strong influence of inhibitor concentration on the electrochemical performance of the TTD.

Key words: thiadiazole; adsorption; corrosion; stainless steel; inhibitor; HCl

1 Introduction

Austenitic stainless steels especially type 304 grades are extensively applied in the process and petroleum industries as a result of their excellent corrosion resistance, due to the protective film formed on their surface when subjected to corrosive industrial conditions. However, exposure to chloride ions under these conditions results in localized corrosion reactions and deterioration [1–3]. HCl acid is widely used for the processing of specific industrial intermediates and materials and in the removal of undesirable scale and rust in metal working, such as cleaning of boilers, heat exchangers and metal extraction [4–6]. The dilute electrolytic phase in the overhead condenser, resulted from the brine water in the crude and steam stripping in petroleum refining, contains mostly HCl acid which is released by hydrolysis of $CaCl_2$ (calcium chloride) and $MgCl_2$ (magnesium chloride) and also contains H_2S (hydrogen sulfide) [7–8]. The corrosion in this unit is mostly due to condensed HCl acid [9–10]. Due to the inherent corrosive nature of acid, the most cost-effective means of corrosion control is with the use of chemical compounds to inhibit the electrochemical process responsible for corrosion. These compounds known as inhibitors are used for controlling the corrosion of metals and alloys in severe environments [11–14].

A significant number of researches have been done on the use of organic compounds as inhibitors for stainless steel corrosion in corrosive acid media, however, 2-amino-5-ethyl-1, 3, 4-thiadiazole (TTD) has not been used to inhibit stainless steel corrosion but has been tested on other metallic alloys with satisfactory results. TTD was evaluated as a corrosion inhibitor for copper in 3% NaCl solutions [15]. The results show that TTD is a good mixed-type inhibitor for copper corrosion and its inhibition efficiency decreases in the order of oxygenated > aerated > de-aerated 3.0% NaCl solutions. The effects of TTD derivative on copper corrosion in aerated acidic pickling solution of 0.5 mol/L HCl acid were investigated using gravimetric and electrochemical techniques [16]. The results of potentiodynamic polarization experiments show a large decrease in cathodic, anodic, and corrosion currents due to the presence of the organic molecules. The corrosion inhibition of TTD for brass in natural seawater was evaluated by potentiodynamic polarisation and electrochemical impedance spectroscopic techniques [17]. It was found that the inhibition efficiency of the thiadiazole derivative increased with the increase in concentration. TTD and 5-propyl-2-amino-1, 3,

Received date: 2015−03−18; **Accepted date:** 2015−06−12
Corresponding author: Roland T. Loto; Tel: +23−48084283392; E-mail: tolu.loto@gmail.com

4-thiadiazole were studied for their influence on the inhibition of corrosion of mild steel in HCl acid [18]. The inhibition efficiency of these compounds varied with the inhibitor concentration, immersion time, acid concentration and solution temperature. They exhibited good inhibition efficiency for mild steel in the acid solution. TTD was evaluated as inhibitors for mild steel in 20% formic acid and 20% acetic acid by mass loss, potentiodynamic polarization and electrochemical impedance techniques. The inhibition efficiency of the compound was found to vary with the inhibitor concentration, immersion time, temperature and acid concentration [19]. The compound is mixed type inhibitors in both acid solutions. The corrosion inhibition efficiencies of TTD and five other TTD derivatives namely 2-amino-5-methyl-1,3,4-thiadiazole, 2-amino-5-n-propyl-1,3,4-thiadiazole, 2-amino-5-hepthyl-1,3,4-thiadiazole, 2-amino-5-undecyl-1,3,4-thiadiazole, and 2-amino-5-tridecyl-1,3,4-thiadiazole were evaluated in the system carbon steel−1 mol/L H_2SO_4 through potentiodynamic polarization and SEM analysis [20]. The results showed that the compounds displayed mixed inhibition properties involving blockage of the steel surface by inhibitor molecules by a Langmuir-type adsorption process. Generally, the results reveal that corrosion inhibition of organic compounds is basically due to adsorption of atoms and molecules of the compounds to the metal surface [21]. This research aims to contribute to the use of organic compounds for corrosion inhibition through the corrosion evaluation of TTD on austenitic stainless steel (type 304) in HCl solution.

2 Materials and methods

2.1 Material

Austenitic stainless steel (type 304) was the steel electrode used for the research, sourced from the open market and analyzed at the Applied Microscopy and Triboelectrochemical Research Laboratory, Department of Chemical and Metallurgical Engineering, Tshwane University of Technology, South Africa. It showed an average nominal composition of mainly 18.11% Cr, 8.32% Ni and 68.32% Fe. The steel sample was cylindrical in shape with a diameter of 18 mm.

2.2 Inhibitor

A colorless and solid flake TTD obtained in synthesized form from SMM Instrument, South Africa was used as the inhibiting compound. The structural formula of TTD is shown in Fig. 1. The molecular formula is $C_4H_7N_3S$, and the molar mass is 129.18 g·mol^{-1}.

TTD solution was prepared in volumetric concentrations of 0.125%, 0.25%, 0.375%, 0.5%, 0.625% and 0.75% respectively per 200 mL of the test solutions.

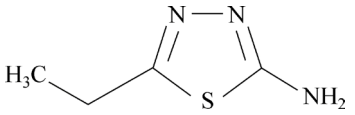

Fig. 1 Chemical structure of 2-amino-5-ethyl-1, 3, 4-thiadiazole

2.3 Test solution

3 mol/L HCl acid with 3.5% recrystallised NaCl (0.6 mol/L NaCl) of analar grade was prepared by dilution of an analytical grade HCl solution (37%) with distilled water and used as the simulated test environment.

2.4 Preparation of test specimens

The cylindrical stainless steel rod (diameter of 18 mm) was mechanically cut into a number of test specimens with length ranging from 17.8 mm to 18.8 mm. The surface ends of each specimen were metallographically prepared with silicon carbide abrasive papers of 80, 120, 220, 800 and 1000 grits before being polished with 6.0 μm to 1.0 μm diamond paste, washed with distilled water, rinsed with acetone, dried and later stored in a dessicator for further mass-loss, open circuit potential and linear polarization tests at the final surface roughness of 1.0 μm.

2.5 Mass-loss experiments

Mass test specimens were separately and fully immersed in 200 mL of the dilute test solutions for 360 h at ambient temperature of 25 °C. Each test specimen was taken out every 72 h, washed with distilled water, rinsed with acetone, dried and re-weighed. Plots of mass-loss (mg) and corrosion rate R (mm/y) versus exposure time T for the test media and those of inhibition efficiency (η) (calculated) versus exposure time T and TTD concentration were made based on experimental measurements of specimen mass. After the tests, the surface roughness of samples changed significantly.

The corrosion rate (R) calculation is defined as [22]

$$R = \frac{87.6m}{DAT} \tag{1}$$

where m is the mass loss in mg, D is the density in g/cm^3, A is the total area in cm^2 and 87.6 is a constant.

Inhibition efficiency η is calculated from the relationship as

$$\eta = \frac{m_1 - m_2}{m_1} \tag{2}$$

where m_1 and m_2 are the mass loss in the absence and presence of predetermined TTD concentrations. η is calculated for all the inhibitors every 72 h during the course of experiment.

The surface coverage is calculated from the relationship [23–24]:

$$\theta = 1 - \frac{m_2}{m_1} \tag{3}$$

where θ is the amount of TTD compound, adsorbed per gram of the stainless steel, m_1 and m_2 are the mass losses of austenitic stainless steel coupon in the absence and presence of TTD in HCl solutions, respectively.

2.6 Open circuit potential measurement

A two-electrode electrochemical cell with silver/silver chloride electrode was used as the reference electrode. The measurements of open circuit potential (OCP) were obtained with Autolab PGSTAT 30 ECO CHIMIE potentiostat (Metrohm Autolab B. V, South Africa). Resin mounted test electrodes/specimens with exposed surface of 254 mm^2 were fully and separately immersed in 200 mL test media (HCl acid) at specific concentrations of TTD for a total of 288 h. The potential of each test electrode was measured every 48 h. Plots of potential (mV) versus immersion time T for the test media are shown in Fig. 6.

2.7 Linear polarization resistance

Linear polarization measurements were carried out with cylindrical steel electrodes embedded in resin plastic mounts with exposed surface of 254 mm^2. The electrode was prepared with specific grades of silicon carbide paper, polished to 6 μm, rinsed by distilled water and dried with acetone. The studies were performed at ambient temperature with Autolab PGSTAT 30 ECO CHIMIE potentiostat and electrode cell containing 200 mL of electrolyte, with and without TTD compound. A graphite rod was used as the auxiliary electrode and silver chloride electrode (SCE) was used as the reference electrode. The steady state open circuit potential (OCP) was noted. The potentiodynamic studies were then made from –1.5 V vs OCP to +1.5 mV vs OCP at a scan rate of 0.00166 V/s. The corrosion current density (J_{corr}) and corrosion potential (E_{corr}) were determined from the Tafel plots of potential vs log current. The corrosion rate (R) is calculated as

$$R = \frac{0.00327 \times J_{corr} \times E_q}{D} \tag{4}$$

where J_{corr} is the current density in μA/cm^2, D is the density in g/cm^3; E_q is the specimen equivalent mass in grams, and 0.00327 is a constant for corrosion rate calculation in mm/y [25–26]. The inhibition efficiency (η_2) is calculated from corrosion rate values as

$$\eta_2 = 1 - \frac{R_2}{R_1} \tag{5}$$

where R_1 and R_2 are the corrosion rates in the absence and presence of TTD respectively.

2.8 Scanning electron microscopy characterization

The surface morphology of the uninhibited and inhibited stainless steel specimens was investigated after mass-loss analysis in 3 mol/L HCl solutions using Jeol JSM 7600F Field Emission Gun Ultra-High Resolution Scanning Electron Microscope at the Electrochemical & Materials Characterization Research Laboratory, Tshwane University of Technology, Pretoria, South Africa. The SEM micrographs were recorded for analysis.

2.9 X-Ray diffraction analysis

X-ray diffraction (XRD) patterns of the film, corrosion products compounds and complexes formed on the metal surface with and without TTD addition were analyzed using a Bruker AXS D2 phaser desktop powder diffractometer with monochromatic Cu K_α radiation produced at 30 kV and 10 mA, with a step size of 0.03° in 2θ. The measurement program is the general scan exccelerator. Analysis of the steel sample inhibited with TTD was done with PANalytical X'Pert Pro powder diffractometer with X'Celerator detector and variable divergence and receiving slits with Fe filtered Co K_α radiation, while the phases were identified using X'Pert Highscore plus software at the School of Chemical and Metallurgical Engineering, University of the Witwatersrand, South Africa.

2.10 Statistical analysis

Two-factor single level statistical analysis tool with the aid of ANOVA test (F-test) was performed so as to investigate the significant effect of TTD concentration and exposure time on the inhibition efficiency values of the TTD in the acid media.

3 Results and discussion

3.1 Mass-loss measurements

The mass-loss of austenitic stainless steel at specific time intervals, in the absence and presence of TTD concentrations in 3 mol/L HCl acid solution at ambient temperature of 25 °C was studied. The values of mass-loss (m), corrosion rate (R) and the inhibition efficiency (η) are presented in Table 1. It is obvious that the corrosion rates decrease progressively in HCl with the increase in TTD concentration. Figures 2, 3 and 4 show the variation of mass-loss, corrosion rate and inhibition efficiency versus exposure time at specific TTD

concentrations while Fig. 5 shows the variation of η with TTD concentration.

Table 1 Data obtained from mass loss measurements for austenitic stainless steel in 3 mol/L HCl in presence of specific concentrations of TTD at 360 h

Sample	Corrosion rate, R/(mm·y^{-1})	Inhibitor concentration/%	Inhibition efficiency, η_1/%	Mass loss, m
A	17.8959	0	0	4.18
B	9.1599	0.125	40.43	2.49
C	6.8918	0.25	54.5	1.902
D	5.8058	0.375	55.07	1.878
E	5.4437	0.5	66.58	1.397
F	5.3924	0.625	69.55	1.273
G	5.1037	0.75	70.22	1.245

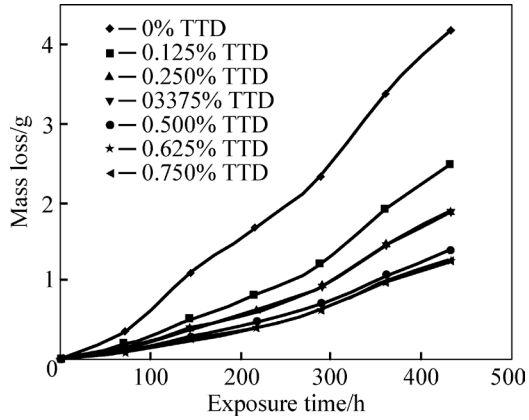

Fig. 2 Variation of mass-loss with exposure time for samples in different TTD concentrations in 3 mol/L HCl

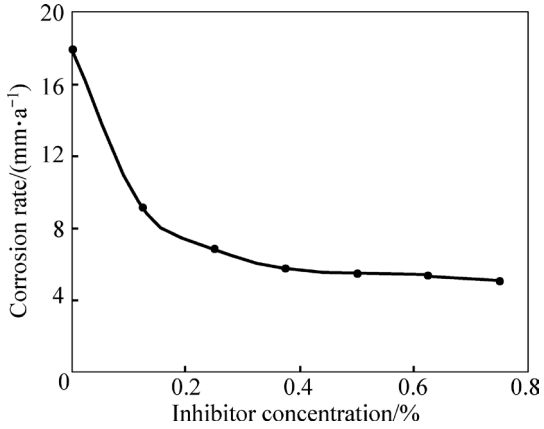

Fig. 3 Effect of concentration of TTD on corrosion rate of austenitic stainless steel in 3 mol/L HCl

The decreased corrosion of the stainless steel is due to the strong adsorption and barrier effect of TTD on the steel surface. The electrochemical reactions within the test solution were significantly altered in the presence of TTD whereby TTD precipitates (reaction products) form a compact barrier which adheres to the metal samples

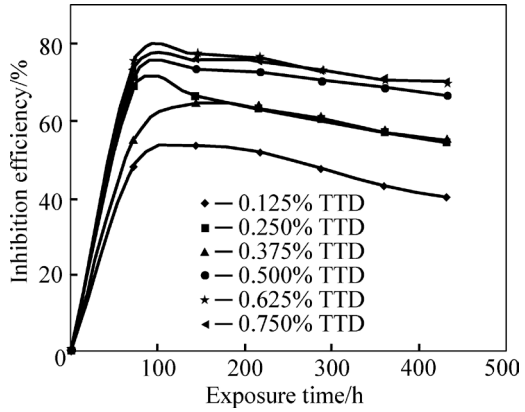

Fig. 4 Plots of inhibition efficiencies of samples versus exposure time in 3 mol/L HCl during exposure period

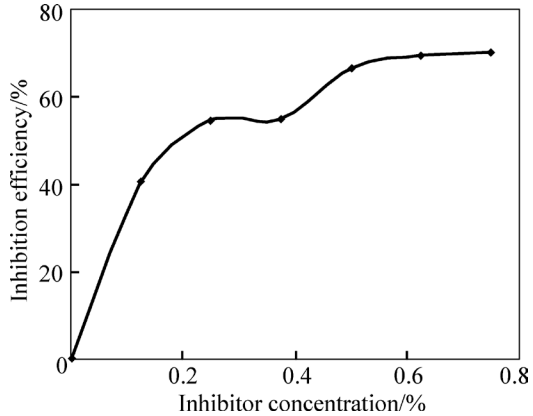

Fig. 5 Variation of inhibition efficiency of TTD versus TTD concentrations from mass loss analysis in 3 mol/L HCl

throughout the exposure period. The reactive sites on the steel surface are thus totally separated from the corrosive species of the HCl acid solution. The compact barrier prevents the diffusion of chloride ions (Cl^-) to the metal surface and simultaneously inhibits metal diffusion into the solution. Within the test solution, the barrier effectiveness varies with TTD concentration due to the availability a number of heterocyclic atoms (N, O and S) in addition the number of functional groups which allows for covalent bonding with the steel, i.e. chemisorption, the process of which will be discussed later. At very low concentrations, TTD underperforms in 3 mol/L HCl, however the η values progress upwardly with the increase in TTD concentrations, thus η is dependent on TTD concentrations. The values of η and corrosion rates prove TTD to be an effective inhibitor for further analysis by other corrosion monitoring techniques.

3.2 Open circuit potential measurement

The open-circuit potential (corrosion potential) of the specimen electrodes is observed for a total of 288 h in 3 mol/L HCl solution as shown in Fig. 6 respectively in the absence and presence of specific concentrations of TTD inhibitor at specific TTD concentrations (0%–0.25%

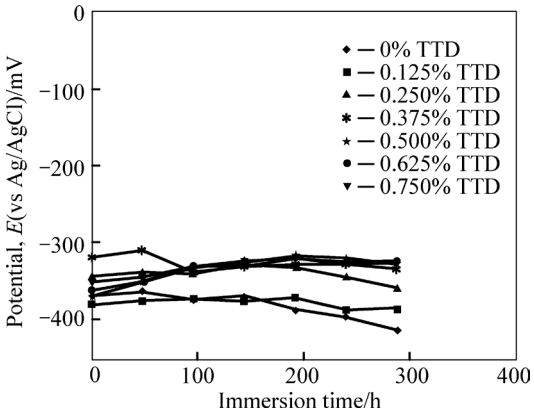

Fig. 6 Variation of potential with immersion time for potential measurements in 3 mol/L HCl

TTD). At (0.125%–0.25%) TTD, the corrosion is reduced very slightly, 0.375%–0.75% TTD concentration results in potential shift to more noble values progressively, due to the effective inhibiting action of TTD. The average potential at these concentrations is about –328 mV which is within passivity values, but the corrosion risk is intermediate. The overwhelming presence of chloride ions quickly destroys the passive film and the amount of TTD molecules is insufficient to inhibit their electrochemical action, but as the concentration of TTD increases, there is a corresponding decrease in corrosion rate till the TTD concentration at which corrosion is effectively inhibited.

3.3 Polarization studies

Potentiostatic potential was cursorily examined from –1.5 V to +1.5 V (vs Ag/AgCl) at a scan rate of 0.00166 mV/s for equilibrium state analysis. The effect of the addition of TTD on the redox polarization curves of austenitic stainless steel (type 304) in 3 mol/L HCl solutions was studied at atmospheric temperature (Fig. 7). The corrosion inhibition of TTD depends on the value of TTD concentration as shown in Fig. 7 due to the delayed

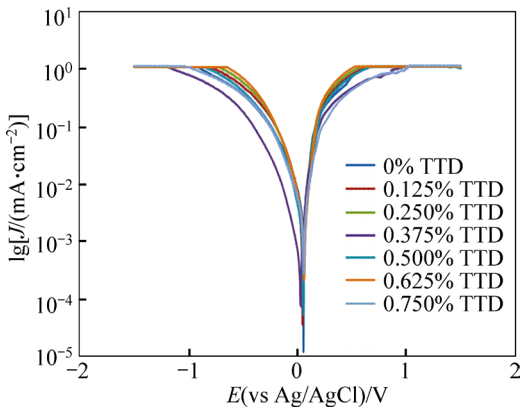

Fig. 7 Comparison of cathodic and anodic polarization scans for austenitic stainless steel in 3 mol/L HCl solution in absence and presence of TTD (0%–0.75%)

action and impact of the inhibitor in preventing the diffusion of aggressive anions to the metal. In Fig. 7, the corrosion potential shifts towards more negative potentials with the increase in TTD concentration resulting in greater adsorption on the steel. This is proven from the corrosion rate values. The observation can also be attributed to the deposition of TTD cations on the alloy in the form of white precipitates as a result of interaction between the functional sites on the inhibitor and the metal surface which effectively seals the surface against further electrochemical reaction. The Relationship between η and inhibitor concentration for polarization test in 3 mol/L HCl is shown in Fig. 8.

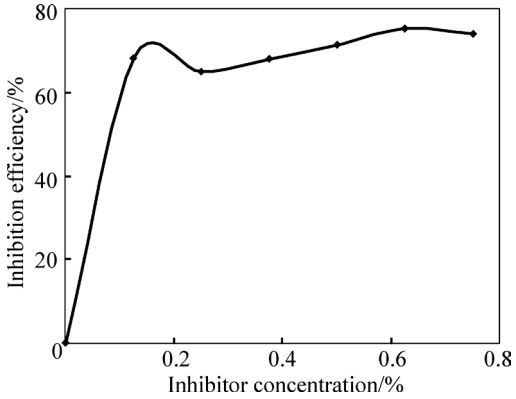

Fig. 8 Relationship between η and inhibitor concentration for polarization test in 3 mol/L HCl

The electrochemical variables such as corrosion potential (E_{corr}), corrosion current (I_{corr}), corrosion current density (J_{corr}), cathodic Tafel constant (B_c), anodic Tafel constant (B_a) and inhibition efficiency (η_2) were calculated and given in Table 2. The corrosion current density (J_{corr}) and corrosion potential (E_{corr}) were determined by the intersection of the extrapolating anodic and cathodic Tafel lines. η_2 is calculated by

$$\eta_2 = 1 - \frac{R_2}{R_1} \tag{6}$$

The maximum displacement of corrosion potential in HCl is –36 mV in the cathodic direction [27–28], thus conventionally it is a mixed type inhibitor. This was confirmed in Refs. [15–18] which studied the corrosion inhibition of copper in NaCl solution and in Ref. [19] which studied the corrosion inhibition of steel in sulphuric acid solution. The mechanism of inhibition being cathodic is due to the suppression of hydrogen evolution and oxygen reduction reactions as a result of TTD adsorption onto the metal surface. Anodic dissolution is effectively inhibited through the formation of a compact barrier (Fig. 9(d)) that prevents ions diffusion and acid solution. In the test solutions, the values of anodic and cathodic Tafel constants show a sharp change with the addition of TTD compound. This

Table 2 Data obtained from polarization resistance measurements for austenitic stainless steel in 3 mol/L HCl at specific concentrations of TTD

Sample	Inhibitor concentration/%	B_a/ (V/dec)	B_c/ (V/dec)	E_{corr}/V	J_{corr}/ (10^{-4}A·cm^{-2})	I_{corr}/ (10^{-4} A)	Corrosion rate, R/(mm·a^{-1})	R_p/ (Ω·cm^2)	Inhibition efficiency, η_2/%
A	0	0.014	0.021	−0.301	5.09	12.9	5.81	2.82	0
B	0.125	0.130	0.038	−0.337	1.62	4.12	1.85	31.03	68.1
C	0.25	0.870	0.039	−0.317	1.78	4.52	2.03	35.90	65.1
D	0.375	0.038	0.230	−0.337	1.62	4.11	1.85	34.50	68.1
E	0.5	0.066	0.081	−0.319	1.46	3.70	1.66	42.73	71.5
F	0.625	0.586	0.036	−0.313	1.26	3.19	1.43	46.23	75.5
G	0.75	0.046	0.144	−0.304	1.34	3.40	1.53	44.58	74.2

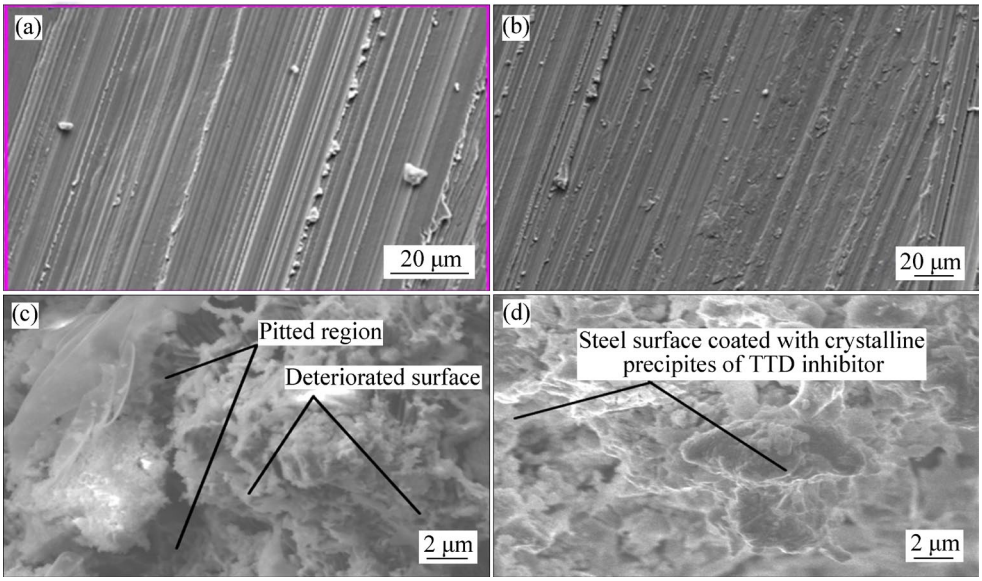

Fig. 9 SEM micrographs: (a) Austenitic stainless steel; (b) Austenitic stainless steel; (c) Austenitic stainless steel in 3 mol/L HCl; (d) Austenitic stainless steel in 3 mol/L HCl with TTD

shows the influence of TTD on the total redox process despite its strong affinity for cathodic reactions. The corrosion current density is also observed to change with the addition of TTD. The linear polarization curves in HCl are generally the same with slight difference in potential displacement. The potentiodynamic polarization experiments carried out by SHERIFF et al [16] show a large decrease in cathodic, anodic, and corrosion currents due to the presence of the organic molecules.

Owing to the strong negative charge of the corrosive anions, competitive adsorption occurs on the steel surface between TTD ions and the corrosive ions due to the positive charge on the surface as a result of oxidation with the preadsorbed chloride ions [29–34]. The preadsorbed anions form chemical complexes of covalent bond with TTD ions through charge transfer and electrochemical interactions with its functional groups through the heterocyclic atoms [35]. The increase in η value in HCl solution is also the result of an increase in the number of adsorbed TTD molecules on the steel, which impedes the diffusion of ions to or from the electrode surface as the degree of surface coverage (θ) increases. The inhibition mechanism of TTD molecules in the solution is predominantly under anodic and cathodic control. Experimental research done by JOSEPH et al [17], QURAISHI et al [18] and RAFIQUEE et al [19] confirmed this observation.

3.4 Scanning electron microscopy analysis

The SEM images of the stainless steel surfaces before and after immersion in 3 mol/L HCl solution with and without TTD addition are given in Figs. 9(a)–(d), respectively. Figures 9(a) and (b) show the steel sample before immersion, the lined surface and serrated edges are due to machining prior to metallographic preparation. Figure 9(c) shows the steel surfaces after 360 h of immersion in 3 mol/L HCl without TTD, while Fig. 9(d) shows the steel surface in the acid media with TTD at maximum concentration. A rough surface is observed in Fig. 9(c); a badly corroded topography of the stainless steel coupons is visible as a result of the corrosive

actions of chloride ions due to the breakdown of the passive film of chromium oxide owing to the high diffusivity of the corrosive ions through cracks on the passive film. The rate of deterioration is faster than the rate of repassivation of the steel surface.

The corrosion attack on the steel specimen is probably due to competitive adsorption/diffusion of Cl^-, whereby the ions diffuse into the metal/liquid interface of the steel surface and displace the passivating species [36]. This is responsible for the uneven topography especially at sites with flaws and inclusions. The passive film is destroyed by the Cl^- ions resulting total exposure to corrosion. The mode of protection of TTD in acid media is due to solid white crystalline precipitates which strongly adheres to the steel through chemisorption mechanism (adsorption) preventing diffusion of Cl^- and Fe^{2+}.

3.5 XRD analysis

The X-ray diffraction (XRD) patterns of the stainless steel surfaces after immersion in 3 mol/L HCl solutions with and without the addition of TTD are shown in Figs. 10(a) and (b) respectively, while the identified patterns are shown in Tables 3 and 4. The peak values at 2θ for the steel specimen in the absence of TTD in the solutions show the presence of phase compounds, i.e. corrosion products, on the steel surface. The peak values at 2θ=39.5° and 50.5° for the steel after immersion in 3 mol/L HCl (Fig.10(a)) correspond to iron (ii) oxide (Fe_2O_3) present on the steel due to corrosion. Observation of the peak values (Fig. 10(b)) on the surface of the steel after immersion in the acid solutions with TTD reveals the absence of (corrosion products) phase compounds. This is probably due to their presence in trace amounts as a result of effective TTD inhibition through film formation. This film keeps the steel surface free of oxides.

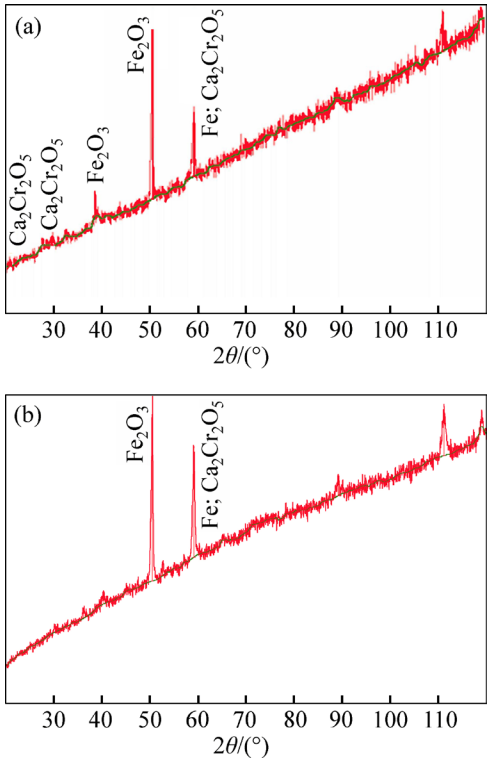

Fig. 10 XRD patterns of surface film formed on austenitic stainless steel after immersion: (a) In absence of TTD in 3 mol/L HCl; (b) In presence of TTD in 3 mol/L HCl

Table 3 Identified patterns list for XRD analysis of austenitic stainless steel in 3 mol/L HCl without TTD

Reference code	Score	Compound	Displacement/ (°)	Scale factor	Chemical formula
01-089-4185	51	Iron	0.312	0.497	Fe
00-048-0791	28	Calcium chromium oxide	0.7	0.058	$Ca_2Cr_2O_5$
01-073-0603	41	Hematite, syn	–0.187	0.032	Fe_2O_3

Table 4 Identified patterns list for XRD analysis of austenitic stainless steel in 3 mol/L HCl with TTD

Reference code	Score	Compound	Displacement/ (°)	Scale factor	Chemical formula
01-088-2323	61	Chromium	–0.478	1.027	Cr
01-087-0722	40	Iron	0.082	0.042	Fe
01-089-4081	37	Sodium	1.204	0.07	Na

3.6 Adsorption isotherm

Corrosion inhibition mechanism can be studied further from adsorption behavior of TTD on the metal surface as it provides insight to the inhibition mechanism in electrochemical reactions. Strong adsorption bond/high surface coverage induced by chemical activity must be the basis of effective inhibition between TTD molecules and the metal surface compared to the interaction between TTD and water molecules. The adsorption of TTD at the metal/solution interface is due to the formation of either electrostatic or covalent bonding between ionized molecules or the metal surface atoms. Freundlich, Frumkin and Langmuir isotherms describe the best experimental results for TTD adsorption in 3 mol/L HCl solutions at 25 °C in the general form:

$$f(\theta, x)\exp(-2a\theta)=KC \quad (7)$$

where $f(\theta, x)$ is the configurational factor which depends upon the physical model and assumption underlying the derivative of the isotherm, θ is the surface coverage, C is the inhibitor concentration, a is the molecular interaction parameter and K is the equilibrium constant of adsorption process.

The general equation for Langmuir isotherm is

$$\frac{\theta}{1-\theta}=K_{ads}C \tag{8}$$

and rearranging gives

$$K_{ads}C=\frac{\theta}{1+K_{ads}\theta}$$

where K_{ads} is the equilibrium constant of the adsorption process. The plots of C/θ versus inhibitor concentration C are linear (Fig. 11) indicating the Langmuir adsorption.

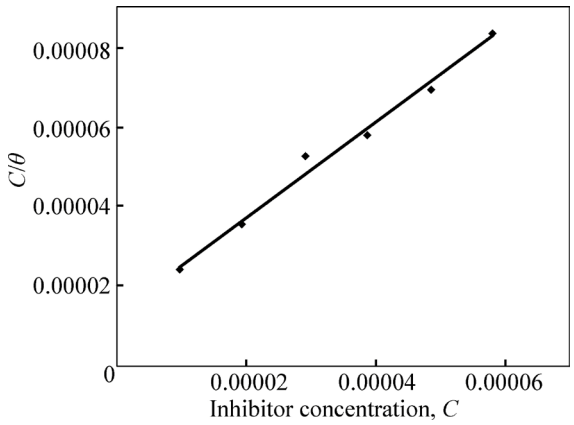

Fig. 11 Relationship between C/θ and inhibitor concentration in 3 mol/L HCl

The divergence of the slope from unity in Fig. 11 is the result of the electrochemical interaction among the adsorbed TTD ions on the metal surface and changes in the values of Gibbs free energy as the surface coverage increases. This is not taken into cognizance when the Langmuir equation is formulated.

Langmuir isotherm states the follows:

1) The metal surface has a definite proportion of adsorption sites with one adsorbate.

2) Gibbs free energy of adsorption has the same value for the sites, independent of the value of surface coverage.

3) There is no evidence of lateral interaction between the adsorbed inhibitor molecules [37].

The fitted lines from the Langmuir equation show values less than unity for the slopes. This suggests a slight deviation from ideal conditions assumed in the equation.

Freundlich isotherm states that the relationship between the amount and concentration of TTD molecules absorbed onto the steel varies at different concentrations [38].

$$\theta=KC \tag{9}$$

$$\lg\theta=n\lg C+\lg K \tag{10}$$

where n is a constant depending on the electrochemical nature of TTD molecule, and $0<n<1$, K is the adsorption-desorption equilibrium constant denoting the strength of interaction in the adsorbed layer. The plot in Fig. 12 fitted according to Eq s. (11) and (12) gives n= 0.127. Positive and large values of K suggest significantly strong interaction between the adsorbed species.

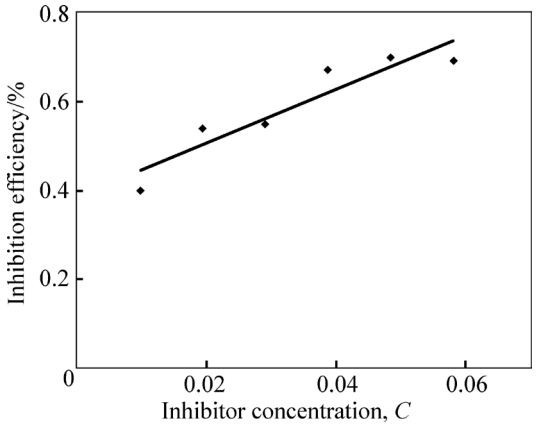

Fig. 12 Relationship between inhibition efficiency and inhibitor concentration in 3 mol/L HCl

Frumkin isotherm assumes unit coverage at high inhibitor concentrations and that the electrode surface is inhomogeneous i.e. the lateral interaction effect is not negligible. In this way, only the active surface of the electrode, on which adsorption occurs, is taken into account. Frumkin adsorption isotherm can be expressed according to

$$\lg[C\times\theta/(1-\theta)]=2.303\lg K+2\alpha\theta \tag{11}$$

where K is the adsorption-desorption constant and α is the lateral interaction term describing the interaction in adsorbed layer. Plots of $\theta/(1-\theta)$ versus inhibitor concentration (C) as presented in Fig. 13 are linear which shows the relevance of Frumkin isotherm. The values for Frumkin adsorption parameters are shown in Table 5. From the result, the lateral interaction term (α) gives declining but positive values suggesting attractive behavior of TTD on the surface of the stainless steel. The

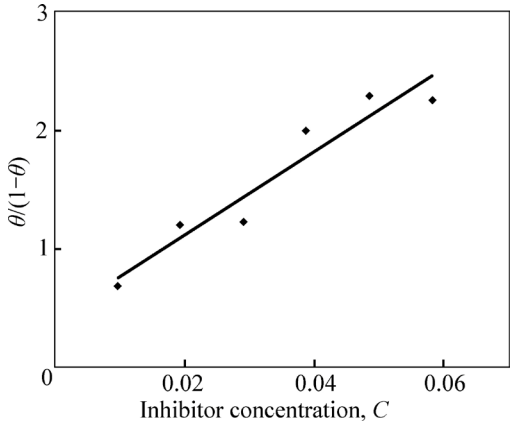

Fig. 13 Relationship between $\theta/(1-\theta)$ and inhibitor concentration (C) in 3 mol/L HCl

Table 5 Relationship between lateral interaction parameter and surface coverage from Frumkin adsorption isotherm

Lateral interaction parameter, α	Surface coverage, θ
1.138	0.404
0.844	0.545
0.835	0.551
0.691	0.666
0.661	0.696
0.664	0.693

α values show that there is strong attraction between TTD molecules resulting in strong adsorption onto the steel surface and high inhibition efficiencies. The slight decline in α is negligible and has no effect on the inhibitive characteristics of TTD.

3.6 Thermodynamics of corrosion process

The values of the apparent free energy change i.e. Gibbs free energy (ΔG_{ads}) for the adsorption process can be evaluated from the equilibrium constant of adsorption using the following equation as shown in Table 6.

$$\Delta G_{ads}=-2.303RT\lg[55.5K_{ads}] \quad (12)$$

where 55.5 is the molar concentration of water in the solution, R is the universal gas constant, T is the absolute temperature and K_{ads} is the equilibrium constant of adsorption. K_{ads} is related to surface coverage (θ) by the following equation.

$$K_{ads}C=\frac{\theta}{1-\theta} \quad (13)$$

The results presented in Table 6 provide additional proof of slight deviation from ideal condition of Langmuir model as observed in the differential values of free energy of adsorption (ΔG_{ads}) with the increase in surface coverage (θ) values. The dependence of free energy of adsorption (ΔG_{ads}) of TTD on surface coverage is ascribed to the heterogeneous characteristics of the metal surface, thus the differential adsorption energies as observed in the experimental data are listed is Table 6. The energy of adsorption depends on factors such as micro pits, slag inclusion, elemental variations, dislocations, and cracks along the grain boundary at the metal surface. Values of ΔG_{ads} around −20 kJ/mol or below are consistent with physisorption characteristics, those of about −40 kJ/mol or above involve charge sharing or transfer between the adsorbate and absorbent to form covalent bonds associated with chemisorption. The value of ΔG_{ads} in HCl shows strong adsorption of TTD to the stainless steel. The negative values of ΔG_{ads} show that TTD adsorption on the metal surface is spontaneous [39–41]. The values of ΔG_{ads} calculated range between 37.60 and 36.14 kJ/mol in HCl solutions.

3.7 Statistical analysis

Two−factor single level experimental ANOVA test (F−test) is used to analyze the separate and combined effects of the concentrations of TTD and exposure time on the inhibition efficiency of TTD in the corrosion inhibition of the stainless steels in 3 mol/L HCl solutions and to investigate the statistical significance of the effects. The F − test is used to examine the amount of variation within each of the samples relative to the amount of variation between the samples.

The sum of squares among columns (exposure time) is obtained as

$$S_{sc}=[(\sum T^2_C/n_r)-(T^2/N)] \quad (14)$$

The sum of squares among rows (inhibitor concentration) is given:

$$S_{sr}=[(\sum T^2_r/n_c)-(T^2/N)] \quad (15)$$

The total sum of squares is given:

$$S_{s,total}=[\sum x^2-T^2/N] \quad (16)$$

The results using the ANOVA test are listed in Table 7.

The statistical analysis in 3 mol/L HCl is evaluated for a confidence level of 95% i.e. a significance level of α=0.05. The ANOVA results (Table 7) in the acid solution reveal the overwhelming influence of inhibitor concentration on the inhibition efficiency with F-value

Table 6 Gibbs free energy, surface coverage and equilibrium constant of adsorption at varying concentrations of TTD in 3 mol/L HCl

Inhibitor concentration/%	Free energy of adsorption, ΔG_{ads}/(kJ·mol^{-1})	Surface coverage/θ	Equilibrium constant of adsorption, K_{ads}	Lateral interaction parameter, α
0	0	0	0	0
0.125	–37.6	0.4043	70141.3	1.138
0.25	–37.29	0.5450	61886.8	0.844
0.375	–36.35	0.5507	42225.4	0.835
0.5	–36.84	0.6658	51468.5	0.691
0.625	–36.62	0.6955	47198.9	0.661
0.75	–36.14	0.6926	38804.3	0.664

Table 7 Analysis of variance (ANOVA) for inhibition efficiency of TTD inhibitor in 3 mol/L HCl (at 95% confidence level)

Source of variation	Sum of squares	Degree of freedom	Mean square	Mean square ratio (MSR)	Minimum of MSR	
					Significance of F	F/%
Inhibitor concentration	7059.73	5	1411.95	139.41	2.71	85.7
Exposure time	743.31	4	185.83	18.35	2.87	8.76
Residual	202.56	20	10.13			
Total	8005.6	29				

of 139.41. These are greater than the significance factor at α=0.05 (level of significance or probability). The F−values of exposure time in solution is less significant compared to inhibitor concentration but greater than the significant factor hence they are statistically relevant with F−values of 18.35. The statistical influence of the inhibitor concentration in HCl is 85.7% while the influence of the exposure time is 8.76%. The inhibitor concentration and exposure time are significant model terms influencing inhibition efficiency of TTD on the corrosion of the steel specimen with greater influence from the concentration of TTD.

4 Conclusions

1) The application of TTD as the corrosion inhibiting compound effectively reduces the corrosion rate of austenitic stainless steel at all concentrations studied from mass loss, potential measurement and potentiodynamic polarization tests.

2) The inhibition efficiency increases in direct proportion to increase in inhibitor concentration due to the availability of more inhibitor molecules to effectively inhibit corrosion until saturation point.

3) The slight deviation of the slopes from unity on the slopes of the adsorption curves is attributed to the molecular interaction among the adsorbed inhibitor species on the metal surface and changes in the values of Gibbs free energy of adsorption with increasing surface coverage.

4) XRD analysis of the stainless steel surface in the solutions without TTD addition shows the presence of iron oxides due to the redox corrosion process that took place on the steel surface. The diffraction peaks for the TTD inhibited steel surfaces show the absence of iron oxides and chemical compounds associated with corrosion.

5) Adsorption of TTD on the stainless steel is found to obey Langmuir, Frumkin and Freundlich adsorption isotherm as it produces the best fit.

6) At a confidence level of 95%, the ANOVA results in test solutions reveal only one of the experimental sources of variation (inhibitor concentration) to be statistically significant on the inhibition efficiency of TTD with F−values of 139.41 and a statistical influence of 85.7% in HCl.

Acknowledgement

The authors acknowledge the Department of Chemical, Metallurgical and Materials Engineering, Faculty of Engineering and the Built Environment, Tshwane University of Technology, Pretoria, South Africa for the provision of research facilities for this work.

References

[1] NIU Li-bin, KENSUKE N. Effect of chloride and sulfate ions in simulated boiler water on pitting corrosion behavior of 13Cr steel [J]. Corrosion Science, 2015, 96: 171–177.

[2] JINA Z H, GEA H H, LINA W W, ZONGB Y W, LIUB S J, SHIC J M. Corrosion behaviour of 316L stainless steel and anti-corrosion materials in a high acidified chloride solution [J]. Applied Surface Science, 2014, 322: 47–56.

[3] TATYANA V S, VERONIKA K L, GALINA A T, ALEXANDER M A, KONSTANTIN V G. The effect of microstructure and non-metallic inclusions on corrosion behavior of low carbon steel in chloride containing solutions [J]. Corrosion Science, 2014, 80: 299–308.

[4] SUDHISH K S, QURAISHI M A. Cefalexin drug: A new and efficient corrosion inhibitor for mild steel in hydrochloric acid solution [J]. Materials Chemistry and Physics, 2010, 120: 142–147.

[5] HMAMOU D B, SALGHI R, ZARROUK A, MESSALI M, ZARROK H, ERRAMI M, HAMMOUTI B, BAZZI L H, CHAKIR A. Inhibition of steel corrosion in hydrochloric acid solution by chamomile extract [J]. Der Pharma Chemica, 2012, 4(4): 1496–1505.

[6] RAPHAEL S O. Corrosion Studies on Stainless Steel (FE6956) in Hydrochloric Acid Solution [J]. Advances in Materials Physics and Chemistry, 2014, 4(8): 153–163.

[7] JAMES G S. Oil and gas corrosion prevention [M]. Houston, US: Gulf Professional Publishing, 2014: 39–66.

[8] Equilibriulm-Stage separation operations in chemical engineering [M]. New York: John Wiley and sons, 1981: 692.

[9] FOROULIS Z A. Corrosion and corrosion inhibition in the petroleum-industry [J]. Materials and Corrosion, 1982, 33: 121–131.

[10] BRIAN C, SRIDHAR S, KWEI M Y, MARK Y. Corrosion in crude distillation unit overhead operations: A comprehensive review [R]. Houston, Texas: NACE International, 2011.

[11] SAVIOUR A U, IME B O, MADHANKUMAR A, ZUHAIR M G. Performance evaluation of pectin as ecofriendly corrosion inhibitor for X60 pipeline steel in acid medium: Experimental and theoretical approaches [J]. Carbohydrate Polymers, 2015, 124: 280–291.

[12] MARÍA E O, JUAN M, GENESCAB J. CO2 corrosion control in steel pipelines. Influence of turbulent flow on the performance of corrosion inhibitors [J]. Journal of Loss Prevention in the Process Industries, 2015, 35: 19–28.

[13] ANSARIA K R, QURAISHIA M A, AMBRISH S. Satin derivatives as a non-toxic corrosion inhibitor for mild steel in 20% H_2SO_4 [J]. Corrosion Science, 2015, 95: 62−70.

[14] PANG X, RAN X, KUANG F, XIE J, HOU B. Inhibiting effect of ciprofloxacin, norfloxacin and ofloxacin on corrosion of mild steel in HCl acid [J]. Chinese Journal of Chemical Engineering, 2010, 18(2): 337–345.

[15] SHERIF E M, SU-MOON P P. 2-Amino-5-ethyl 1, 3, 4-thiadiazole as corrosion inhibitor for copper in 3.0% NaCl solutions, Corrosion Science, 2006, 48(12): 4065−4079.

[16] SHERIF E M, SU-MOON P. Effects of 2-amino-5-ethylthio-1, 3, 4-thiadiazole on copper corrosion as a corrosion inhibitor in aerated acidic pickling solutions. Electrochimica Acta, 2006, 51: 6556–6562.

[17] JOSEPH RA X, RAJENDRAN N. Corrosion inhibition effect of substituted thiadiazoles on Brass [J]. International Journal of Electrochemical Science, 2011, 6: 348−366.

[18] QURAISHI M A, KHAN S. Thiadiazoles- A potential class of heterocyclic inhibitors for prevention of mild steel corrosion in HCl acid solution [J]. Indian Journal of Chemical Technology, 2005, 12(5): 576–581.

[19] RAFIQUEE M Z A, KHAN S, SAXENA N, QURAISHI M A. Influence of some thiadiazole derivatives on corrosioninhibition of mild steel in formic and acetic acid media [J]. Portugaliae Electrochimica Acta, 2007, 25: 419–434.

[20] OCTAVIO O X, NATALYA V L, NOEL N, AGUSTÍN C P, IRINA V L, ESCOBEDO-MORALES A, CLAUDIA L. Thiadiazoles as Corrosion Inhibitors for Carbon Steel in H_2SO_4 Solutions [J]. International Journal of Electrochemical Science, 2013, 8: 735–752.

[21] MESSAADIA L, EL MOUDEN O-ID, ANEJJAR A, MESSALI M, SALGHI R, BENALI O, CHERKAOUI O, LALLAM A. Adsorption and corrosion inhibition of new synthesized Pyridazinium-Based Ionic Liquid on Carbon steel in 0.5 M H_2SO_4 [J]. Journal of Materials and Environmental Science, 2015, 6(2): 598−606

[22] VENKATESAN, P, ANAND, B, MATHESWARAN, P. Influence of formazan derivatives on corrosion inhibition of mild steel in hydrochloric acid medium [J]. Journal of Chemistry, 2009, 6(1): 438–444.

[23] ABBASOVA V M, ABD EL-LATEEFA H M, ALIYEVAA L I, QASIMOVA E E, ISMAYILOVA I T, KHALAF M M. A study of the corrosion inhibition of mild steel C1018 in CO_2-saturated brine using some novel surfactants based on corn oil [J]. Egyptian Journal of Petroleum, 2013, 4(22): 451–470.

[24] SETHI T, CHATURVEDI A, MATHUR R K. Corrosion inhibitory effects of some schiff's bases on mild steel in acid media [J]. Journal of Chilean Chemical Society, 2007, 3(52): 1206–1213.

[25] AHMAD K. Principles of corrosion engineering and corrosion control [M]. Oxford, UK: 2006: 112.

[26] CHOI Y, NESIC S, LING S. Effect of H_2S on the CO_2 corrosion of carbon steel in acidic Solutions [J]. Electrochimical Acta, 2011, 56: 1752–1760.

[27] EDUOK U M, UMOREN S A, UDOH A P. Synergistic inhibition effects between leaves and stem extracts of Sida acuta and iodide ion for mild steel corrosion in 1 M H2SO4 solutions [J]. Arabian Journal of Chemistry, 2010, 5(3): 325–337.

[28] TROWSDALE A, NOBLE J B, HARRIS S J, GIBBINS I S R, THOMPSON G E, WOOD G C. The influence of silicon carbide reinforcement on the pitting behaviour of aluminium. Corrosion Science, 1996, 38(2): 177–191.

[29] FLORIAN B M. Corrosion mechanisms [M]. New York: Mercel Dekker. 1987: 138.

[30] VEDULA S S. Green corrosion inhibitors, theory and practice [M]. John Hoboken, New Jersey: Wiley & Sons Inc, 2011: 208.

[31] PARAMESWARI K, CHITRA S, SELVARAJ A, BRINDHA S, MENAGA M. Investigation of Benzothiazole Derivatives as Corrosion Inhibitors for Mild Steel. Portugaliae Electrochimica Acta, 2012, 30(2): 126–132.

[32] AGARWAL P, LANDOLT D. Effect of anions on the efficiency of aromatic carboxylic acid corrosion inhibitors in near neutral media: Experimental investigation and theoretical modeling. Corrosion Science, 1998, 40: 673–691.

[33] WANG B, DU M, ZHANG J, GAO C J. Electrochemical and surface analysis studies on corrosion inhibition of Q235 steel by imidazoline derivative against CO_2 corrosion, Corrosion Science, 2011, 53: 353–361.

[34] BRETT C M A, GOMES I A R, MARTINS J P S. The electrochemical behaviour and corrosion of aluminium in chloride media. The effect of inhibitor anions [J]. Corrosion Science, 1994, 36: 915–923.

[35] KHAMIS A, SALEH M M, AWAD M I. The counter ion influence of cationic surfactant and role of chloride ion synergism on corrosion inhibition of mild steel in acidic media [J]. International Journal of Electrochemical Science, 2012, 7: 10487–10500.

[36] WINSTON R R. Corrosion and Corrosion Control [M]. Hoboken, New Jersey: John Wiley & Sons Inc, 2008: 99.

[37] VILLAMIL R F V, CORIO P, RUBIN J C, AGOSTINHO S M I, NIU Li-bin, KENSUKE N. Effect of sodium dodecylsulfate on copper corrosion in sulfuric acid media in the absence and presence of benzotriazole [J]. International Journal of Electrochemical Science, 1999, 472: 112–119.

[38] UNUABONAH E, OLU-OWOLABI B, ADEBOWALE O, OFOMAJA E. Adsorption of lead and cadmium ions from aqueous solutions by tripolyphosphate-impregnated Kaolinite clay [J]. Colloids and Surface A: Physisochemical Engineering Aspects, 2007, 292: 202–211.

[39] HOSSEINI M G, MERTENS S F L, ARSHADI M R. Synergism and antagonism in mild steel corrosion inhibition by sodium dodecylbenzenesulphonate and hexamethylenetetramine [J]. Corrosion, Science, 2003, 45: 1473–1489.

[40] SOLMAZ R. Investigation of the inhibition effect of 5-((E)-4-phenylbuta-1,3-dienylideneamino)-1,3,4-thiadiazole-2-thiol Schiff base on mild steel corrosion in HCl acid [J]. Corrosion Science, 2010, 52(10): 3321–3330.

[41] DÖNER A, SOLMAZ R, ÖZCAN M, KARDAŞ G. Experimental and theoretical studies of thiazoles as corrosion inhibitors for mild steel in sulphuric acid solution. Corrosion Science, 2011, 53(9): 2902–2913.

(Edited by FANG Jing-hua)